Mathematical aspects of BRDF modeling: adjoint problem and Green's function

Y. Knyazikhin[1] and A. Marshak[2]

[1]Department of Geography, Boston University
675 Commomwealth Avenue, Boston, MA 02215
Tel.: (617) 353 8843; Fax: (617) 353 8399;
E–mail: jknjazi@crsa.bu.edu

[2]Climate and Radiation Branch
NASA/Goddard Space Flight Center, Code 913
Greenbelt, MD 20771
Tel.: (301) 614–6122, Fax: (301) 614–6307
Email: marshak@climate.gsfc.nasa.gov

Abstract – Adjoint formulation of three–dimensional radiative transfer and the Green's function concept have been developed in neutron transport several decades ago. This is not merely yet another method of simulating the radiative transfer process, but a method of reformulating the problem to better incorporate existing radiation models into a particular research. In the case of photon transport in vegetation canopies, the Green's function is a canopy radiative response to a point monodirectional source located outside the canopy. The Green's function, therefore, has intrinsic canopy information. It can be evaluated by using existing canopy radiation models. The problem–dependent adjoint formulation of radiative transfer allows us to express a particular canopy radiation effect in terms of the Green's function and, as a consequence, to better adjust the existing models to the solution of a specific radiation problem. Application of this technique to the retrieval of biophysical parameters from remotely sensed data (the table look–up method) was discussed in (Kimes et al., this issue). In this paper, we will illustrate how this concept can be applied to the estimation of cloud optical properties from ground–based measurements of spectral zenith radiance above the vegetation canopy under broken cloud conditions. In spite of different physical formulations of these problems, both of them use the Green's function to describe radiation fields due to the interaction between the canopy ground and the canopy and the canopy–clouds interaction. This technique allows us not only to extend an applicability range of existing canopy–radiation models, but also to incorporate of various approaches developed in other fields of physics into BRDF modeling and its applications.

Keywords – Green's function, adjoint problem, conservative model

1. INTRODUCTION

Land surface processes are important components of the terrestrial climate system. Accurate descriptions of the interaction between the surface and the atmosphere require reliable quantitative information on the fluxes, mass, and momentum, especially over terrestrial areas, where they are closely associated with the rates of evapotranspiration and photosynthesis. Many of these processes can be related to the spectral reflectance of the surface. The vegetation canopy

is classified as a special type of surface not only due to its role in the energy balance but also due to its impact on the global carbon cycle. Its reflection results from bio−physiological, chemical and physical processes, and is characterized by spatial, seasonal and diurnal variations. The three−dimensional incoming radiation field and three−dimensional structure of vegetation canopies determine these spatial and temporal variations which influence various physiological and physical processes required for the functioning of plants. Therefore these models that describe the three−dimensional radiation field in vegetation canopies and the three−dimensional radiation field of incoming radiation as well as the interaction between these fields are required by many interdisciplinary researches.

Because of the complexity and ambiguity in the interpretation of both satellite images and ground based measurements of the solar radiation in the presence of broken clouds, scientists prefer to deal with either clear or overcast skies. For example, land scientists use clear sky data for estimating land cover and vegetation indices while atmospheric scientists would rather analyze overcast sky data for retrieving optical and geometrical properties of clouds. As a result, a large amount of data that show a complex three−dimensional structure of both clouds and vegetation is at best substantially underexploited.

The main objectives of this paper is to demonstrate a technique developed in neutron transport which allows us to accurately account for features of three-dimensional radiation fields in designing algorithms for estimation of cloud optical properties from ground−based measurements above the vegetation canopy under broken cloud conditions. Application of the same technique to the retrieval of biophysical parameters from remotely sensed data was discussed by (Kimes et al., this issue). In spite of different physical formulations of these problems, both of them use the same technique to describe radiation field due to (1) the interaction between the canopy ground and the canopy and (2) the canopy−clouds interaction. This technique allows us not only to extend an applicability range of existing canopy−radiation models, but also to incorporate of various approaches developed in other fields of physics into BRDF modeling and its applications.

2. EXPANSION OF THE THREE−DIMENSIONAL RADIATIVE FIELD

Let us consider a three−dimensional scattering and absorbing medium. This medium can be either a vegetation canopy or a cloudy layer. The monochromatic intensity $I_\lambda(r,\Omega)$ of a three−dimensional radiation field at wavelength λ, at a spatial point r and in direction Ω can be represented as a sum of two components; that is,

$$I_\lambda(r,\Omega) = I_{\mathrm{bs},\lambda}(r,\Omega) + I_{\mathrm{rest},\lambda}(r,\Omega). \tag{2.1}$$

The first component, $I_{\mathrm{bs},\lambda}$, describes the radiative regime within the medium for the case of a black surface underneath the medium ("standard problem"), and $I_{\mathrm{rest},\lambda}$ describes additional radiative field due to the interaction between the underlying surface and the medium.

It is well known (e.g., Chandrasekhar, 1960, p. 273; van de Hulst, 1980, p. 64; Stamnes, 1982, Box et al., 1988) that in the case of simple slab geometry and a Lambertian surface with albedo $\rho_{\mathrm{sur},\lambda}$, the additional term can be expressed as

$$I_{\text{rest},\lambda} = \frac{\rho_{\text{sur},\lambda}}{1 - \rho_{\text{sur},\lambda} R_\lambda} F_{\text{bs},\lambda} I_{\text{S},\lambda} . \tag{2.2}$$

Here λ denotes wavelength; $F_{\text{bs},\lambda}$ is the downwelling flux at the medium bottom for the standard problem; $I_{\text{S},\lambda}$ is the solution to the transport equation with a normalized isotropic source $Q_\text{S} = 1/\pi$ (in sr^{-1}) located at the medium bottom, and R_λ is the downwelling flux at the medium bottom generated by Q_S. Thus one needs three independent variables to describe the radiative regime in the plane−parallel medium. They are (1) reflectance properties of the underlying surface, which do not depend on the medium; (2) $I_{\text{bs},\lambda}$ and (3) $I_{\text{S},\lambda}$, which are surface independent parameters since no multiple interaction of radiation between the medium and underlying surface is possible, i.e., these variables have intrinsic canopy information.

Somewhat more complicated techniques, adjoint formulation and Green's function concept, have been developed in reactor physics to extend the representations (2.1) and (2.2) for the case of three−dimensional radiation fields (Bell and Glasstone, 1970). Although in the three-dimensional case $I_{\text{rest},\lambda}$ cannot be expressed in such a simple form, the physical meaning of (2.1) and (2.2) remains unchanged; that is, a three−dimensional radiation field can be expressed in terms of ground reflectance properties which are independent on the medium; the radiation field in the medium bounded at the bottom by a black surface; and the radiation field in the medium generated by anisotropic heterogeneous wavelength−independent sources located at the surface underneath the medium. Though this technique has been developed in the neutron transport several decades ago (Bell and Glasstone, 1970), it has only recently been incorporated into an operational algorithm for retrieval of bio−physical parameters from canopy reflectance data provided by the MODIS (Moderate Resolution Imaging SpectroRadiometer) and MISR (Multi−angle Imaging SpectroRadiometer) instruments aboard the Earth Observing System Terra. (Knyazikhin et al., 1998a,b; Kimes et al., this issue).

3. PHOTON INTERACTION BETWEEN CLOUDS AND VEGETATIONS

It is well recognized that clouds vary both vertically and horizontally. Solar radiation reflected from or transmitted through clouds is affected by these variabilities. As a result, measured radiation includes convoluted information on both intrinsic cloud properties and radiative effects of three−dimensional cloud structure. However, almost all radiative transfer calculations that interpret satellite or ground−based measurements assume that clouds vary only vertically, ignoring not only horizontal in−cloud structure but also broken cloudiness. This can lead to misinterpretation of cloud properties. In this section we illustrate the effects of cloud inhomogeneity on ground−based measurements of zenith radiances in the visible (VIS) and near−IR (NIR) spectral regions. Then, we show that a simple algebraic combination of these independent measurements can partly remove the ambiguity in the interpretation of measured downwelling zenith radiances caused by a horizontally inhomogeneous cloud structure. A simple example will explain the role of spectral contrast in green vegetation in removing this ambiguity.

3.1. Three−dimensional radiation effects of broken clouds

In Fig. 1a we plotted a 1000 sec data stream of simulated zenith radiances transmitted through a broken cloud field and "measured" by upward−looking radiometer with 5 sec averaging.

Assuming a 5 m/sec wind speed, this can be also interpreted as a 5 km fragment of zenith radiance measured with 25 m resolution (thus the horizontal axis notations is in km). In addition to the field of zenith radiances, in Fig. 1b we plotted a 5 km fragment of a stochastic model of cloud optical depth that corresponds to the radiances from panel (a). Canopy BRDF was simulated using the RPV model (Rahman et al., 1993).

First of all, we see a clear signature of tiny cloudy pixels (e.g., around 9.5 and 11 km); next, we see a strong increase in brightness around cloud edges (11.2 km) and shadows behind them (11.4 km). For large optical thicknesses (from 8 to 8.8 km and 12.2 to 13 km), we observe much smoother behavior of zenith radiances than the corresponding cloud field. This is so called "radiative smoothing" (Marshak et al., 1995) – a process that is determined by multiple scattering and photon horizontal transport. To conclude, there are two competing radiative processes: shadowing (or "roughening") and smoothing; while the shadowing makes fluctuations larger, the smoothing suppresses them.

All these three-dimensional radiative effects violate a one–to–one relationship between optical depth and zenith radiances and make it absolutely impossible to retrieve cloud optical thicknesses at a pixel–by–pixel basis. Figure 1c illustrates this with a scatter plot of 10240 points of zenith radiances calculated by the Monte Carlo method for 10 realizations of a stochastic cloud model plotted vs. cloud optical depth. (The 5 km fragment in Fig. 1a with 200 points is extracted from one of these realizations).

Wavenumber spectrum, as a Fourier transform of an autocorrelation function (e. g., Papoulis, 1965), is a very informative characterization of fluctuations in both cloud liquid water and zenith radiance fields. Figure 1d illustrates two wavenumber spectra: on the upper curve, there is cloud optical depth (to be retrieved), while on the lower curve, measured zenith radiances. The lower spectrum clearly illustrates the dependence of the above mentioned three-dimensional radiative effects on scale. If the wavenumber spectrum $E(k)$ of optical depth τ is a power low,

$$E(k) \sim k^{-\beta} \ , \tag{3.1}$$

with a spectral exponent $\beta \approx 1.4$, the spectrum of zenith radiances has much more complex structure. For the large and intermediate scales (from ≈ 0.5 km to 20 km), its wavenumber spectrum flattens indicating more energy (larger fluctuations); for small scales, the spectrum steepens indicating smaller fluctuations. Note that the former is a signature of radiative shadowing while the latter characterizes radiative smoothing.

In order to use zenith radiances for estimating cloud optical properties, one has to remove the three-dimensional radiative effects of horizontal variability (shadowing and smoothing). As long as fluctuations of cloud optical thicknesses and measured radiation are different at a certain scale, it is impossible to reliably retrieve optical thickness at this scale. Thus, as a necessary (but not sufficient) condition for the retrieval of cloud optical properties from the radiances transmitted through broken clouds, one should find a nonlinear transformation that makes wavenumber spectra similar to those of the optical depth field down to a certain scale. In the next subsection, we demonstrate a simple transformation that partially removes three-dimensional radiative effects and generates the desired wavenumber spectra.

3.2. A nonlinear transformation

It is well known that because of chlorophyll in the live green leaves, vegetation strongly absorbs solar radiation in the visible spectral region. In contrast, around 0.8 µm green leaves absorb relatively little and the hemispherical reflectance of vegetation often exceeds 50%. Vegetation (or spectral) indices that exploit this spectral contrast in surface reflectance are typically used in analyzing and compressing satellite data. Amongst more than a dozen such indices (Verstraete and Pinty, 1996), the Normalized Difference Vegetation Index (NDVI) between the NIR and red spectral regions is, perhaps, the most widely used by scientific community, since it detects the presents of green (live) vegetation (Tucker, 1979).

By analogy with NDVI, we define a Normalized Difference Cloud Index (NDCI) as the ratio between the difference and the sum of two zenith radiances, I_{NIR} and I_{VIS}, measured for two narrow spectral bands in the VIS and NIR spectral regions and normalized by the TOA (Top of Atmosphere) solar irradiance $F_{0,\lambda}$ at the corresponding wavelengths

$$\text{NDCI} = \frac{I_{NIR} - I_{VIS}}{I_{NIR} + I_{VIS}} \quad . \tag{3.2}$$

3.3. An example

Figure 2a shows a 5 km fragment of measured zenith radiances at two wavelengths in the VIS (the same as in Fig. 1a) and NIR spectral regions. Figure 2b is identical to Fig. 1b which is added here for better visualization. The model of (Rahman et al., 1993) was used to simulate the canopy spectral BRDF. The bold black curve is the NDCI defined in (3.2). We see that NDCI is much more sensitive to cloud structure than either zenith radiances and shows the monotony with respect to cloud optical thickness. A scatter plot (Fig. 2c) yields the best illustration of the monotonic dependence of NDCI on τ. While zenith radiance $I_{NIR}(\tau)$ is strongly effected by three-dimensional radiative effects, NDCI(τ) can be well approximated by a linear function, at least for $\tau < 40$. Figure 2e shows the histogram of [NDCI(τ)–Linear_fit(τ)] which exhibits Gaussian type behavior with more than 70% points between −0.025 and 0.025.

Finally, the improvement is confirmed by the wavenumber spectra (Fig. 2d). The wavenumber spectra of NDCI has the same slope as its cloud optical depth counterpart down to about $r = 0.4$ km; below this scale, NDCI(x) is smoother than τ (x) which is clearly seen if one compares Figs. 2a and 2b. This means that averaged over a 0.4 km scale both NDCI and τ have similar fluctuations (autocorrelation function); thus cloud optical depth can be successfully retrieved at this scale.

4. THEORETICAL BASIS FOR DESIGNING OF NDCI

4.1. Scale invariant models of horizontal cloud structure

Fractal (scale invariant) models can be used to simulate horizontal distribution of cloud optical thickness (Schertzer and Lovejoy, 1987; Cahalan, 1994, Marshak et al., 1994). These models reproduce the statistics and scale invariance (3.1) observed for cloud liquid water in marine Stratocumulus (Cahalan and Snider, 1989, Davis et al., 1996, Marshak et al., 1997). These

properties can be simulated using a simple three–parameter fractal model called a "bounded cascade." Besides average optical depth (parameter $<\tau>$), this model controls scaling behavior of cloud liquid water (spectral exponent β), and its variance–to–mean ratio (parameter p). As any cascades (Mandelbrot, 1977), this model starts with a homogeneous slab of optical depth $<\tau>$, then transfers a fraction that depends on both parameters β and p from one half to the other in a randomly chosen direction. The same procedure is repeated recursively at ever smaller scales (Cahalan, 1994). As a result, after a few cascade steps we have a rich structure of horizontal distribution of cloud liquid water; its fluctuations obey Eq. (3.1) with β typically from 1.3 to 1.6 (Davis et al., 1996).

Figures 1b and 2b show a small fragment of a bounded cascade model with parameters $<\tau>=13$, $\beta=1.4$, and $p = 0.35$ which are typical for marine stratocumulus. Inner cloud structure is supplemented with gaps using a simple procedure described by Marshak et al. (1998). The upper curves in Figs. 1d and 2d illustrate the wavenumber spectrum of the resulting optical depth field averaged over 10 realizations of a cascade model.

4.2. Difference in spectral properties of green leaves and clouds

The hemispherical leaf albedo is the portion of radiation flux density incident on the leaf surface that the leaf transmits or reflects. The typical spectral variation of leaf albedo (Fig. 3) is defined by three distinct spectral regions (Walter–Shea and Norman, 1991), i.e., VIS (0.4 − 0.7 μm), NIR (0.7 − 1.35 μm), and mid–IR (1.35 − 2.5 μm). If in the visible region 90−95% of solar radiation is absorbed by a single leaf, in the NIR region it absorbs only 5−10% (the rest radiation is either reflected or transmitted, ≈45−50% each). The hemispherical leaf albedo in the mid–IR region is usually smaller than in the NIR. These properties are inferred from the spectral behavior of a green, healthy leaf, and are quite stable although the magnitude of reflectance and transmittance may vary with leaf age and among species. In addition to single leaf spectral properties, the spectral reflectance is determined by canopy structure which is also a stable characteristic of a given site (Ross, 1981, Myneni et al., 1989). Simple functions which relate optical properties of individual leaves and the canopy structure to canopy spectral reflectance are presented in (Knyazikhin et al., 1998a; Panferov et al., 1999).

In contrast to vegetation, cloud optical properties do not change much between 0.5 and 0.9 μm. For the sake of simplicity, the single scattering albedo, ϖ_0, phase function asymmetry parameter, g, and extinction coefficient, σ, are assumed to be constant in this spectral region. We also assume that different amount of the Rayleigh scattering in this region can be removed using a simple atmospheric correction. In addition, we assume a weak wavelength dependence in the optical properties of aerosol in this region. As a result, the red (0.65 μm) and NIR (0.86 μm) wavelengths would be assumed to have the same cloud optical properties but totally different surface reflectances. In general, the above assumptions are not valid. However, the violation of these assumptions have a much smaller effect on zenith radiances than the effect of a contrast between canopy reflectances at red and NIR.

To get larger contrast in surface albedo, it is of interest to use an ozone free UV wavelength, for instance, $\lambda_1=0.38$ μm, where the surface is even more absorbing (95−98%) but Rayleigh scattering is also very strong. Assuming again that cloud optical properties at 0.38 μm and 0.86 μm are similar, and the effect of Rayleigh scattering can be accurately removed, we can count on this UV wavelength as a prototype of a "black" surface.

4.3 Surface–clouds interaction

In this sub–section we will use a schematic plot (Fig. 4) to illustrate the photon interaction between clouds and vegetation. For the sake of simplicity, we assume that a vegetation canopy underneath a three–dimensional cloudy layer can be idealized as a horizontally homogeneous Lamebrain surface. It should be noted that this assumption is not essential for the following analysis (Knyazikhin et al., 1998a). Using adjoint radiative transfer (e.g., Bell and Glasstone, 1970), it can be shown that the surface–cloud interaction term in Eq. (2.1) can be expressed as a product of $\rho_{\text{sur},\lambda}$ and an integral over the whole underlying surface of the downward flux F_λ and a radiative transfer Green's function G, i.e.,

$$I_{\text{rest},\lambda}(r,\Omega) = \rho_{\text{sur},\lambda} \int F_\lambda(r')G(r,\Omega;r')\,dr' \tag{4.1}$$

Here

$$G(r,\Omega;r') = \int_{2\pi^-} G_0(r,\Omega;r',\Omega')|\mu'|\,d\Omega'$$

where G_0 is the Green's function which describes the cloud radiative response to the point monodirectional source $Q_0 = \delta(\Omega-\Omega')\delta(r-r')$ at a spatial point r' of the underlying surface. The function $G(r,\Omega;r')$ can be treated as a cloud radiative response at a spatial point r and in direction Ω on the illumination from below by the isotropic source $Q_S = \pi^{-1}\delta(r-r')$ located at the point r'. Integrating (2.1) over downward directions and accounting for (4.1) result in

$$F_\lambda(r_0) = F_{\text{bs},\lambda}(r_0) + \rho_{\text{sur},\lambda} \int R(r_0,r')F_\lambda(r')\,dr' \tag{4.2}$$

Here r_0 denote a spatial point of the surface underneath the three–dimensional cloudy layer; $R(r_0,r')$ is the downwelling flux at the point r_0 generated by the isotropic source Q_S. Under conditions formulated in section 4.2, the variables G, R and $F_{\text{bs},\lambda}/F_{0,\lambda}$ do not depend on λ. Here $F_{0,\lambda}$ is the TOA solar irradiance. In the case of simple slab geometry (i.e., R, $F_{\text{bs},\lambda}$ and F_λ do not depend on r_0 and r'), the representation (2.2) can be obtained by averaging (4.1) and (4.2) over the underlying surface and resolving the obtained equations with respect to mean values of $I_{\text{rest},\lambda}$ and F_λ.

This is similar to a Davis et al.'s (1997) idea of illuminating clouds by a laser beam, as a Dirac δ–function, and measuring the resulting "spot size," as a radiative transfer Green function. Based on diffusion approximation, in the case of a slab geometry, Davis et al. (1997) were able to analytically derive the relationship between cloud optical and geometrical thicknesses, from one side, and the spot size, from the other.

4.4. NDCI

Since canopy reflectance varies considerably between VIS and NIR while cloud optical properties can be assumed constant, the difference between two normalized zenith radiances I_{NIR},

and I_{VIS}, measured at the same location is equal to the difference between surface−clouds interaction at the same wavelengths, i. e.,

$$I_{NIR} - I_{VIS} = I_{rest,NIR}/F_{0,NIR} - I_{rest,VIS}/F_{0,VIS} \qquad (4.3)$$

Normalizing Eq. (4.3) by the sum of the same normalized radiances, we get the NDCI defined in Eq. (3.2). If the downward flux F is available, it is preferable to use it for normalization [see Eqs. (4.1) and (4.2)]. As a result, we get another NDCI, which better describes the surface−clouds interaction where the surface serves as a diffusive wavelength independent source of photons that illuminate horizontally variable clouds (Fig. 4). Equations (4.1) and (4.2) can be taken as a basis for designing other spectral indices.

The evaluation of the NDCI is similar to the satellite nadir measurements in the sense that both the NDCI and the satellite register photons emitted by a known source and reflected by clouds. This suggests that the NDCI contains a lot of information on intrinsic cloud properties. In other words, with the help of NDCI, we can study cloud optical and geometrical properties using the surface as a powerful wavelength−independent reflector.

5. DISCUSSIONS AND RESEARCH PRIORITIES

The efficiency of any modeling technique must be measured against its ability to address important scientific objectives. Requirements of various scientific communities to products of BRDF models/data are discussed in this special issue. Among others, a very important task is to provide correct relationships between BRDF and environmental variables (e.g., canopy structure, cloud optical depth, etc.). Does an ideal BRDF model exist which can fully represent the suite of variables causing the observed variation in the directional reflectance distribution of plant canopies? We start our analysis with a theorem recently published in a journal on inverse problems (Choulli and Stefanov, 1996). This theorem states that under some general conditions, the three−dimensional extinction coefficient and the three−dimensional scattering phase function can be uniquely retrieved from boundary measurements. It should be noted, however, that its validity is lost in the case of two or one−dimensional media. This theorem indicates that there is a one−to−one correspondence between the complex three−dimensional vegetation canopy structure and radiation emergent from the canopy boundaries. A question then arises whether or not this correspondence can be specified. Let us consider a hypothetical ideal instrument which can provide ideally exact BRDF at any spatial point and in any direction, i.e., one has the complete and accurate spatial and angular information on the radiation field leaving the canopy through the upper boundary. The theorem, however, requires information on the upward radiation field at the canopy bottom boundary in order to recover canopy structure. How can this information be obtained?

A specific feature of photon interaction with vegetation lies in the fact that the probability that a photon will interact with phytoelement does not depend on wavelength; that is, the extinction coefficient, which is the sum of wavelength dependent scattering and absorption coefficients, does not depend on wavelength (Ross, 1981). This property allows us to evaluate canopy transmittance at any wavelength once this variable is known at a fixed wavelength (Knyazikhin et al., 1998a; Panferov et al., 1999). This allow us to mathematically formulate the problem of the link between the three−dimensional canopy structure and the BRDF, namely, given "ideal" multiangle canopy reflectances at a minimum of two spectral bands to find the

canopy transmittance at a fixed wavelength and canopy structure. This formulation includes two sets of known data and two sets of unknowns, which relate all variables needed for unique retrieval of the three–dimensional structure of the medium. It is clear that the above arguments need a rigorous mathematical analysis.

The above arguments indicate that the canopy radiation model, which is the foundation of any BRDF, must also provide canopy transmittance in order to obtain a closed system of equations describing a one–to–one correspondence between biophysical parameters and radiation emergent from the canopy boundaries. The use of the energy conservation law is a most natural and physically well justified approach to introduce this variable into the model. A radiative transfer model is defined to be conservative if the law of energy conservation holds true for any elementary volume (Bass et al., 1986). Within a conservative model, radiation absorbed, transmitted, and reflected by the canopy is always equal to radiation incident on the canopy. However a rather wide family of canopy radiation models designed to account for the hot spot effect conflict with the law of energy conservation (Knyazikhin et al., 1998a). Therefore, the success of development of BRDF models and their applications depends, to a high degree, upon being able to derive a canopy transport equation which, from the one hand, allows for the hot spot effect, and, from the other hand, is conservative. Technique discussed here and in (Kimes et al., this issue) was applied to two different physical problems, namely, estimation of optical properties of broken clouds and remote sensing of vegetation canopies. In spite of different physical formulations of these problems, both of them use the Green's function to describe radiation field due to the interaction between the canopy ground and the canopy and the canopy–clouds interaction. However this technique presupposes the use of conservative radiative transfer models. Therefore, the derivation of a conservative transport equation in vegetation canopies will help us not only to develop more sophisticated radiative transfer models, but also to promote incorporation of various approaches developed in other fields of physics into BRDF modeling and its applications. And this paper aims to demonstrate it.

References

Bass, L.P., A.M.Volocsvhenko, and T.A.Germogenova, 1986: Methods of Discrete Ordinates in Radiation Transport Problems (in Russian, with English abstract), Inst. Appl. Math., Russ. Acad. of Sci., Moscow, 231 pp.

Bell, G. I., and Glasstone, 1970: Nuclear Reactor Theory, Van Nostrand Reinholt, New York, 619 pp.

Box, M. A., S. A. W. Gerstl, and C. Simmer, 1988: Application of the adjoint formulation of the calculation of atmospheric radiative effects. Beitr. Phys. Atmosph., 61, 303–311.

Cahalan, R. F., 1994: Bounded cascade clouds: Albedo and effective thickness. Nonlinear Processes in Geoph., 1, 156–167.

Cahalan, R. F., and J. B. Snider, 1989: Marine stratocumulus structure during FIRE. Remote Sens. Environ., 28, 95–107.

Chandrasekhar, S., 1950: Radiative Transfer, Oxford University Press, reprinted by Dover, 1960, New York (NY), 393 pp.

Choulli, M., and P. Stefanov, 1996: Reconstruction of the coefficient of the stationary transport equation from boundary measurements, Inverse Problems, 12, L19–L23.

Davis, A., A. Marshak, R. Cahalan, and W. Wiscombe, 1997: The LANDSAT scale–break in stratocumulus as a three–dimensional radiative transfer effect, implications for cloud remote sensing. J. Atmos. Sci., 54, 241– 260.

Davis, A., A. Marshak, W. Wiscombe, and R. Cahalan, 1996: Scale–invariance in liquid water distributions in marine stratocumulus, Part I, Spectral properties and stationarity issues. J. Atmos. Sci., 53, 1538–1558.

Kimes, D., Y. Knyazikhin, J. Privette, A. Abuelgasim, and F. Gao, 1999: Inversion methods for physically–based models, Remote Sensing Reviews, this issue.

Knyazikhin, Y., J. V. Martonchik, R. B. Myneni, D. J. Diner, and S. W. Running, 1998a: Synergistic algorithm for estimating vegetation canopy leaf area index and fraction of absorbed photosynthetically active radiation from MODIS and MISR data. J. Geophys. Res., 103, 32257–32275.

Knyazikhin, Y., J. V. Martonchik, D. J. Diner, R. B. Myneni, M. M. Verstraete, B. Pinty, and N. Gobron, 1998b: Estimation of vegetation canopy leaf area index and fraction of absorbed photosynthetically active radiation from atmosphere–corrected MISR data. J. Geophys. Res., 103, 32239–32256.

Mandelbrot, B. B., 1977: Fractals: Form, Chance, and Dimension, 365 pp., W. H. Freeman, San Francisco (Ca).

Marshak, A., A. Davis, R. F. Cahalan, and W. J. Wiscombe, 1994: Bounded cascade models as non–stationary multifractals. Phys. Rev. E, 49, 55–69.

Marshak, A., A. Davis, W. J. Wiscombe, W. Ridgway, and R. F. Cahalan, 1998: Biases in shortwave column absorption in the presence of fractal clouds. J. Climate, 11, 431–446.

Marshak, A., A. Davis, W. Wiscombe, and R. Cahalan, 1995: Radiative smoothing in fractal clouds. J. Geophys. Res., 100, 26,247–26,261.

Marshak, A., A. Davis, W. Wiscombe, and R. Cahalan, 1997: Scale–invariance of liquid water distributions in marine stratocumulus, Part 2 – Multifractal properties and intermittency issues. J. Atmos. Sci, 54, 1423– 1444.

Myneni, R. B., J. Ross, and G. Asrar, 1989: A review on the theory of photon transport in leaf canopies in slab geometry. Agric. For. Meteorol., 45, 1–165.

Panferov, O., Y. Knyazikhin, R.B. Myneni, J. Szarzynski, S. Engwald, K. G. Schnitzler, and G. Gravenhorst, 1999: The role of canopy structure in the spectral variation of transmission and absorption of solar radiation in vegetation canopies, *IEEE Trans. Geosci. Remote Sens.,* (submitted for publication).

Papoulis, A., 1965: Probability, Random Variables, and Stochastic Processes. McGraw–Hill, New York (NY), xi+583pp.

Rahman, H., B. Pinty, and M.M Verstraete, 1993: Coupled surface–atmosphere model reflectance model (CSAR) model 2. Semiempirical surface model usable with NOAA Advance Very High Resolution Radiometer data. J. Geophys. Res., 98, 20791–20801.

Ross, J., 1981: The Radiation Regime and Architecture of Plant Stands, Dr. W. Junk, Norwell, Mass., 391 pp.

Schertzer, D., and S. Lovejoy, 1987: Physical modeling and analysis of rain and clouds by anisotropic scaling multiplicative processes. J. Geophys. Res., 92, 9693–9714.

Stamnes, K., 1982: Reflection and transmission by a vertically inhomogeneous planetary atmosphere. Planet. Space Sci., 30, 727–732.

Tucker, C. J., 1979: Red and photographic infrared linear combination for monitoring vegetation. Remote Sens. Environ., 8, 127–150.

Van de Hulst, H. C., 1980: Multiple Light Scattering: Tables, Formulas, and Applications. Vol. 1., Academic Press, San Diego (Ca).

Verstraete, M. M., and B. Pinty, 1996: Designing optical spectral indexes for remote sensing applications. IEEE Trans. Geoscience Rem. Sensing, 34, 1254–1265.

Walter–Shea, E. A., and J. M. Norman, 1991: Leaf Optical Properties. In Photon–Vegetation Interactions: Applications in Plant Physiology and Optical Remote Sensing, edited by R. B. Myneni and J. Ross, pp. 229– 251. Springer–Verlag, New York.
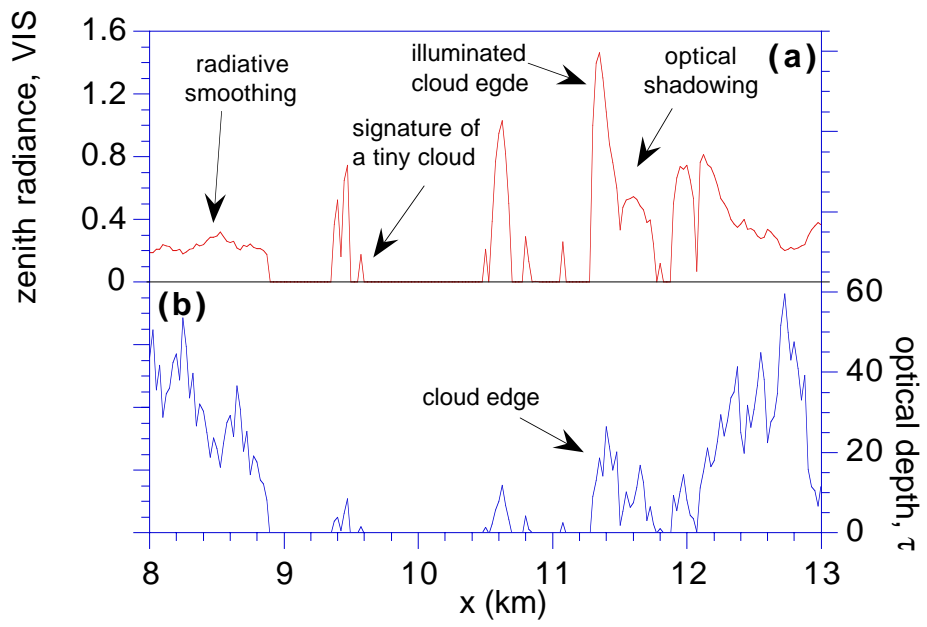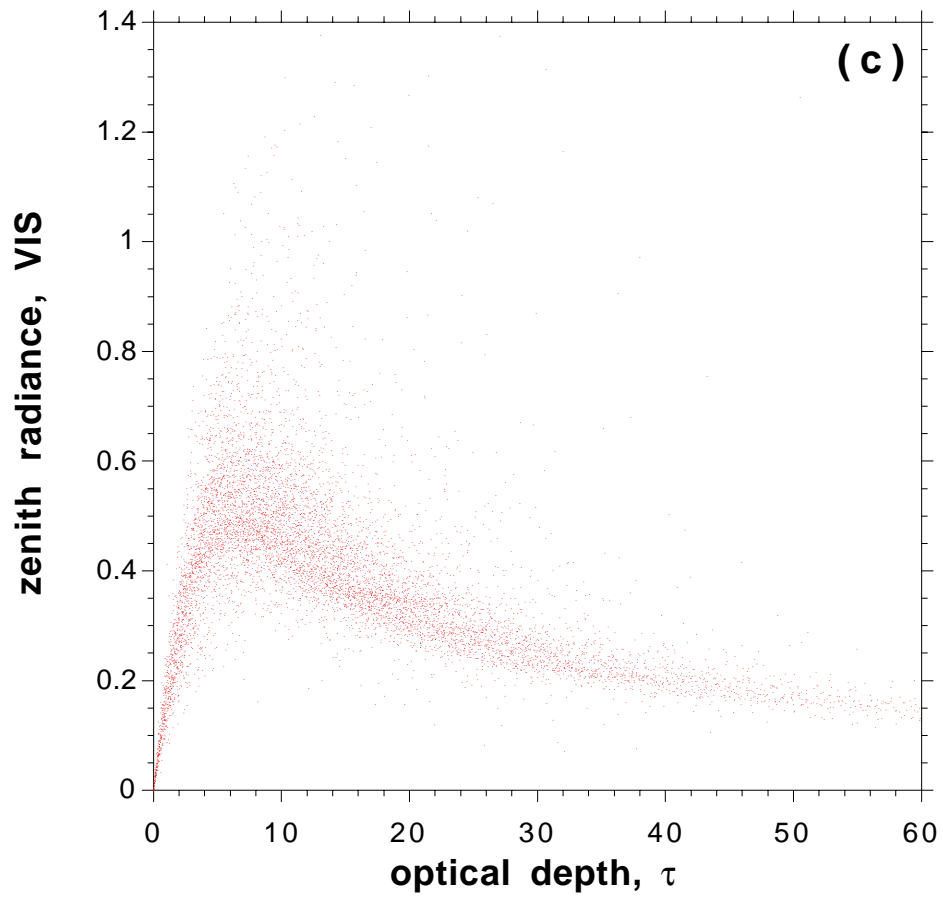
Figure captures

Figure 1: Three-dimensional radiative effects. (a) A 5 km fragment of zenith radiance at a wavelength in the visible spectral region calculated by Monte Carlo method. Pixel size is 25 m, solar zenith angle $\theta_0 = 60^0$, solar azimuth angle $\varphi_0 = 0^0$ (illumination from the left), conservative scattering ($\varpi_0 = 1.0$), Henyey−Greenstein scattering phase function. The RPV model (Rahman et al., 1993) was used to simulate canopy BRDF for irrigated wheat. (b) A 5 km fragment of horizontal distribution of optical thickness, $\tau(x)$, that corresponds to the zenith radiance plotted in panel (a). 10−cascade bounded model (Section 4.1) with parameters $<\tau> = 13$, $\beta = 1.4$ and $p = 0.35$ has been used. Geometrical cloud thickness is 300 m. (c) A scatter−plot of zenith radiance $I^{\downarrow}(\tau)$ vs. τ. 10240 points correspond to 10 realizations of a bounded cascade model. Cloud fraction is 84 %. (d) Wavenumber spectra of 10 realizations of cloud optical depths (above) and zenith radiances (below). A slope $\beta = 1.4$ that corresponds to the spectral exponent of a cloud optical depth model is added for convenience.
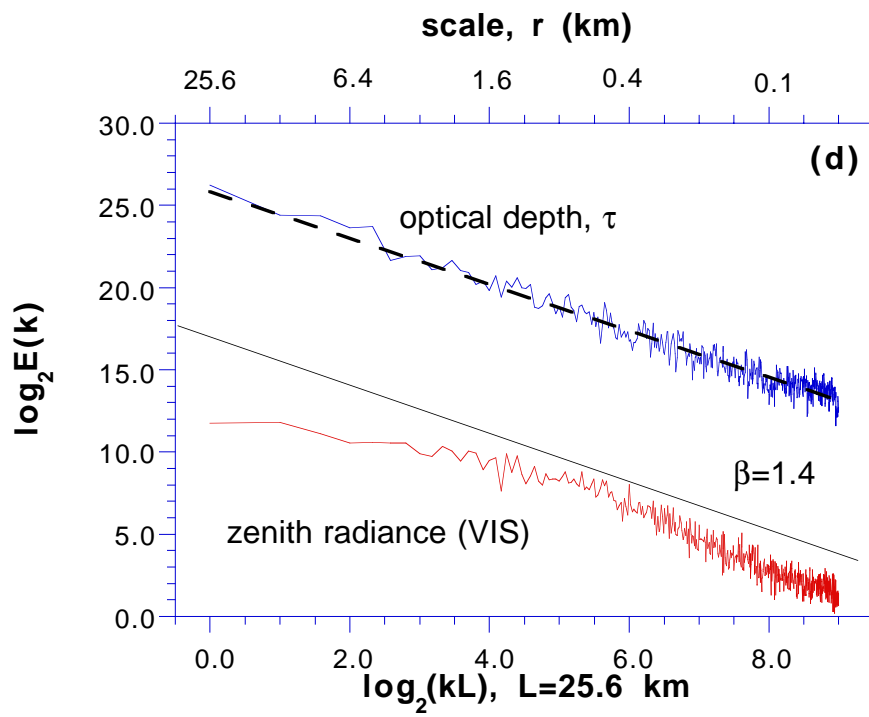
Figure 2: Removal of three-dimensional radiative effects. (a) A 5 km fragment of zenith radiances at two wavelengths in the visible (the same as in Fig. 1a) and near−IR spectral regions. Spectral index NDCI is also shown. Illumination conditions, optical and geometrical parameters of the statistical model of cloud optical depth are the same as in Fig. 1a. (b) A 5 km fragment of horizontal distribution of optical thickness identical to Fig. 1b. (c) A scatter plot of zenith radiances at NIR wavelength (green dots) and the NDCI (black dots) plotted against τ. (d) The same as in Fig. 1d but the wavenumber spectrum of the NDCI is also added. (e) The histogram of the difference between the NDCI and the linear fit; both are plotted in panel (c).
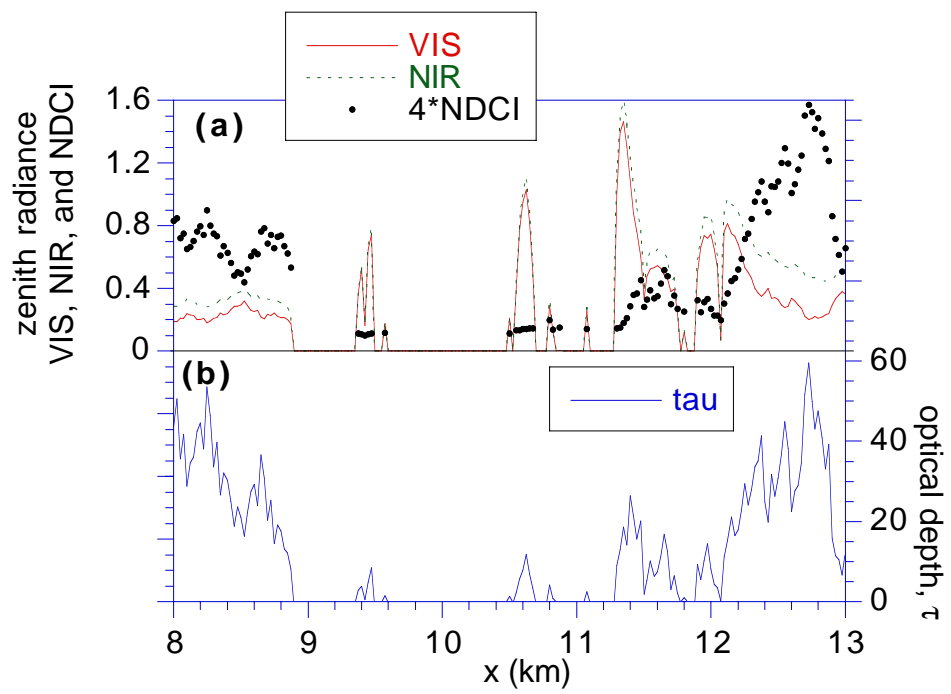
Figure 3: Mean leaf hemispherical albedo of broadleaf forests and its standard deviation as a function of wavelength.

Figure 4: A schematic illustration of surface−clouds interaction. $I^{\downarrow}(r_0) = I_\lambda(r_0, \Omega)/F_{0,\lambda}$ is the normalized zenith radiance at a point r_0 of the surface underneath a cloudy layer; $I^{\downarrow}_{bs}(r_0) = I_{bs}(r_0)/F_{0,\lambda}$ is the normalized zenith radiance at the point r_0 for ideally black surface; $F_{0,\lambda}$ is the solar irradiance spectrum at the top of the atmosphere; $\rho_{sur,\lambda}$ is hemispherical surface reflectance; $T(r') = F_\lambda(r')/F_{0,\lambda}$ is the transmittance of the cloudy layer at a point r' of the surface; $G^{\downarrow}(s) = G(r_0, \Omega; r')$, $s = |r_0 - r'|$, is the cloud radiative response on the illumination by an isotropic source $Q_S = 1/\pi$ located at the point r'.
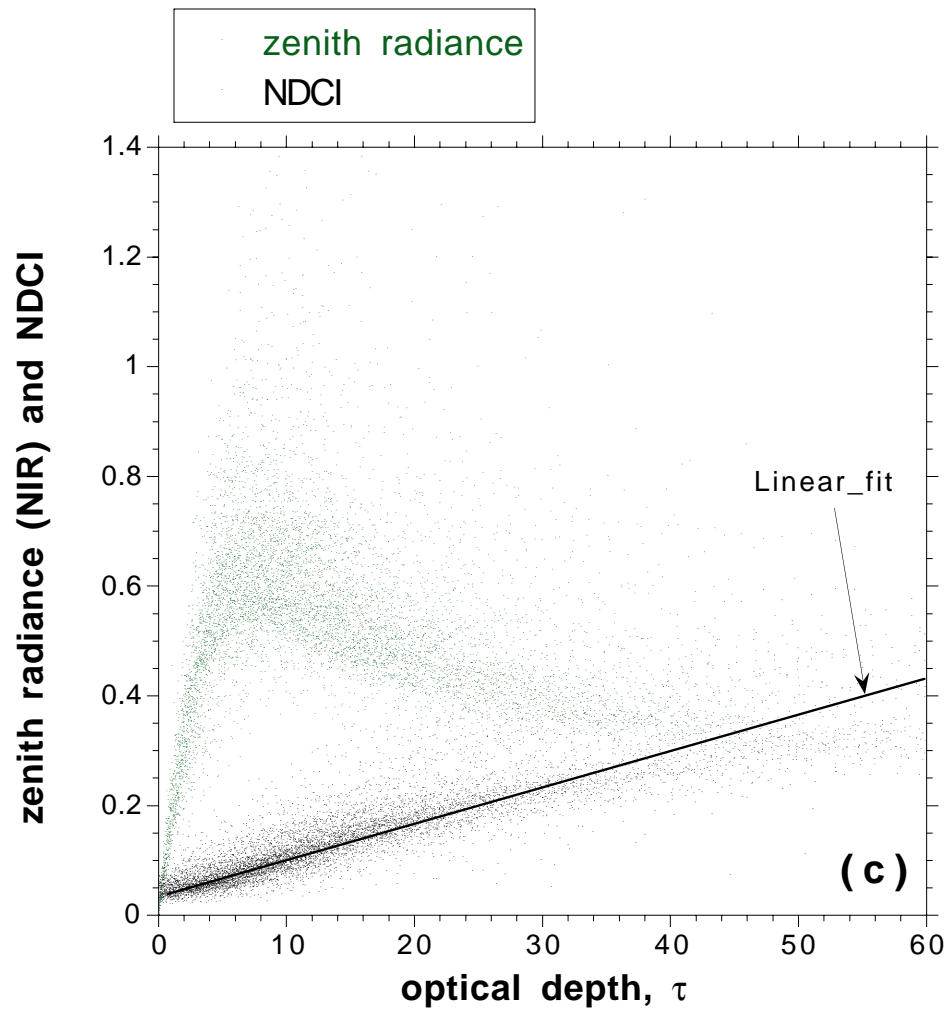
scale, r (km)

optical depth, τ

β=1.4

zenith radiance (VIS)

log₂E(k)

log₂(kL), L=25.6 km

(d)

(d)

scale, r (km)

optical depth, τ

$\beta=1.4$

zenith radiance (VIS)

NDCI

$\log_2 E(k)$

$\log_2(kL)$, L=25.6 km
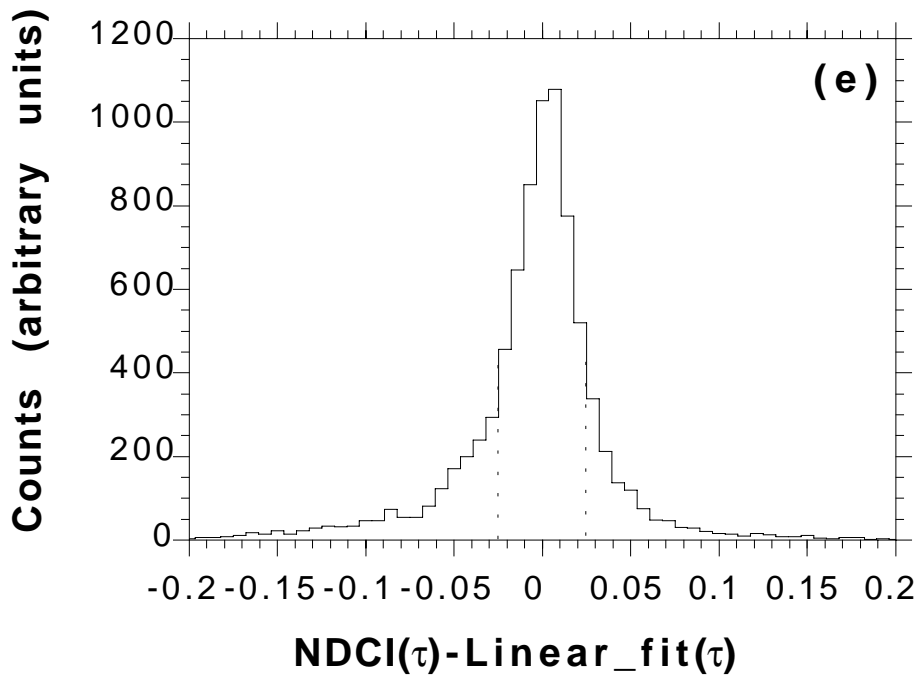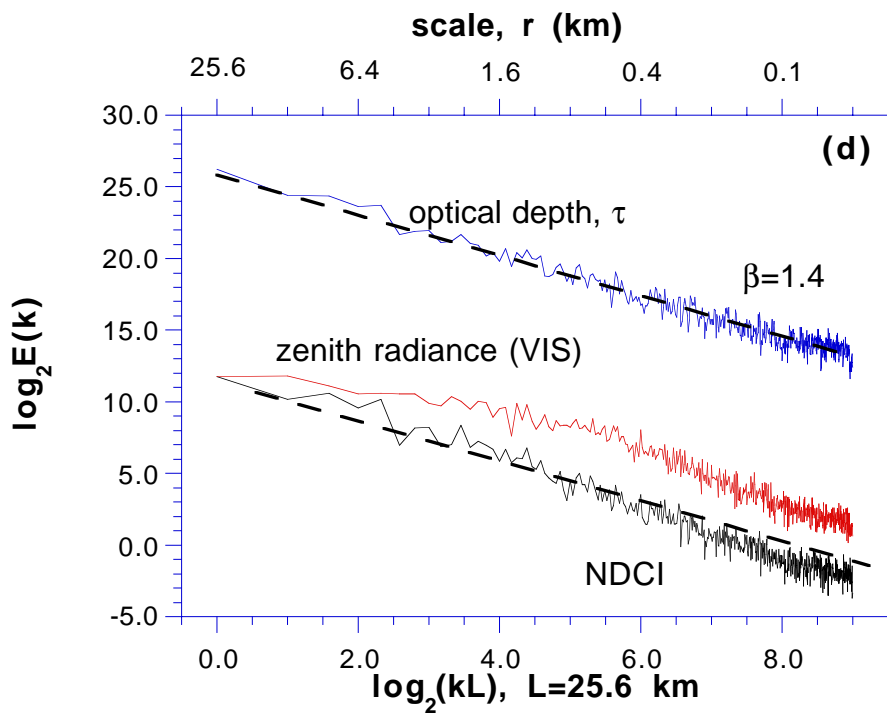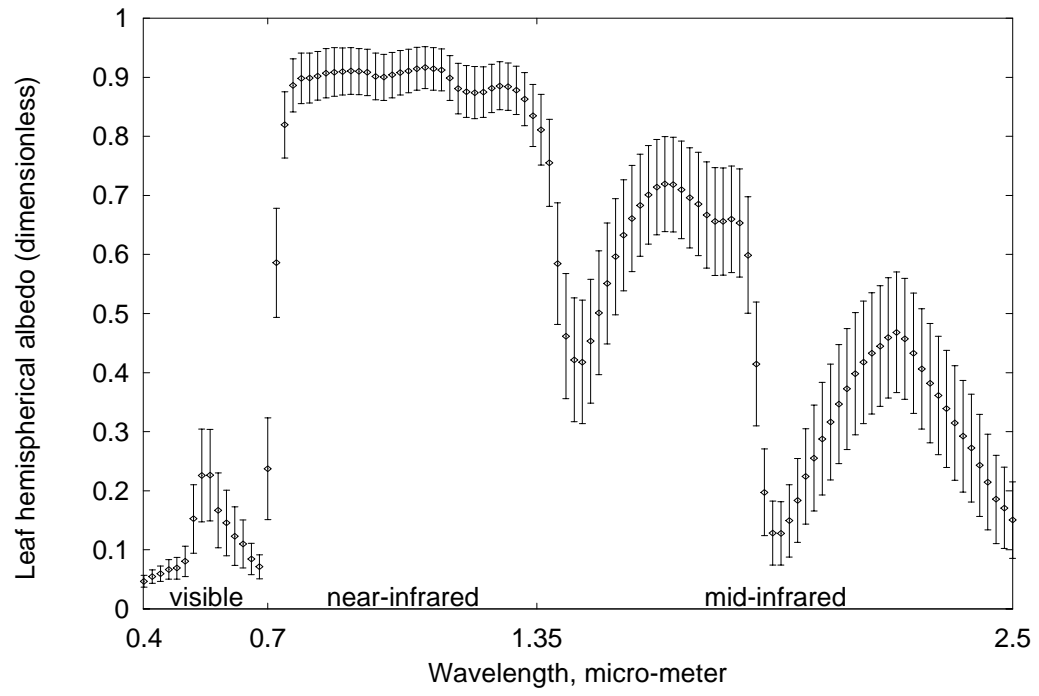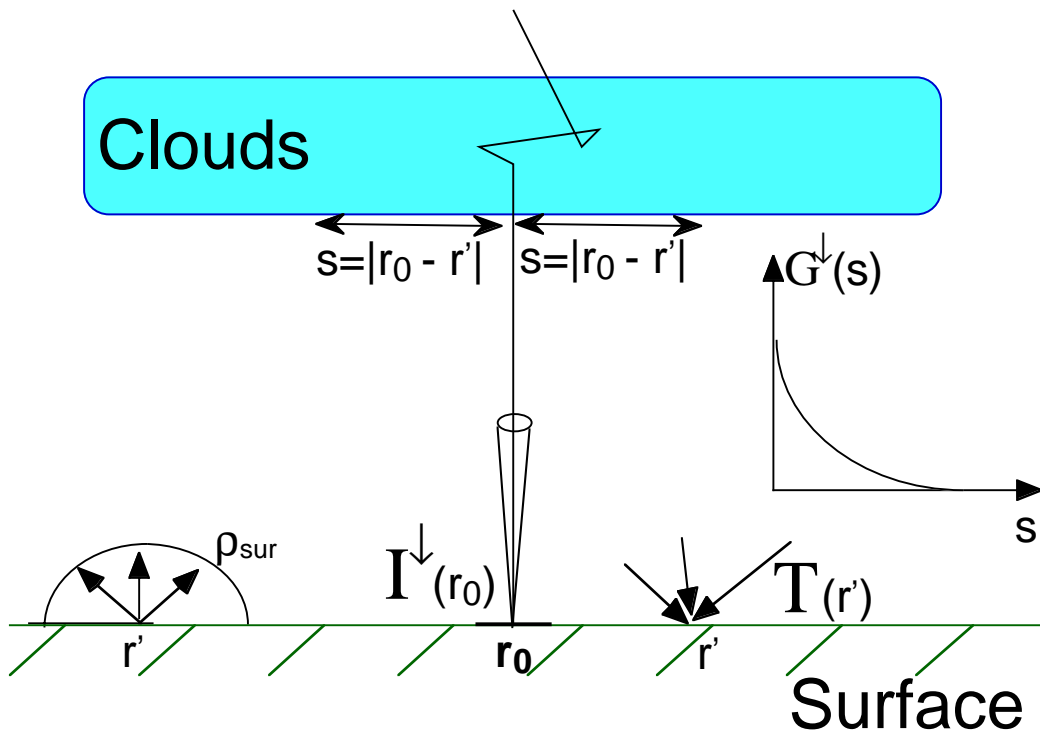
(e)

Counts (arbitrary units)

NDCI(τ)-Linear_fit(τ)

Surface - clouds interaction

$$I^{\downarrow}(r_0) = I^{\downarrow}_{bs}(r_0) + \rho_{sur} \int T(r') G^{\downarrow}(|r_0 - r|) dr'$$

over surface

independent of surface

surface reflectance (independent on clouds)

radiation in clouds generated by illumination from surface